Impact of half-wave plate systematics on the measurement of cosmic birefringence from CMB polarization

Marta Monelli

Max Planck Institut für Astrophysik
Garching (Germany)

December 16th, 2022

CMB anisotropies

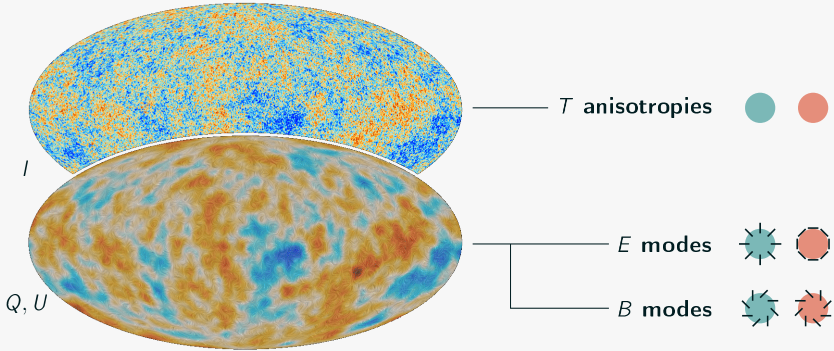

slide adapted from Jonathan Aumont's

searching B-modes from inflation

Expectation: inflation-sourced perturbations leave traces on the CMB polarization.

Large scale B-modes can probe inflation.

Unprecedented sensitivity requirements!

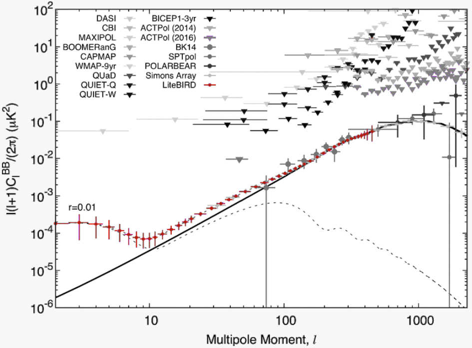

image credit: Hazumi et al (2019)

a side effect: measuring cosmic birefringence

CMB might also carry information about
parity-violating new physics: **cosmic birefringence**.

(time-dependent parity-violating pseudoscalar field)

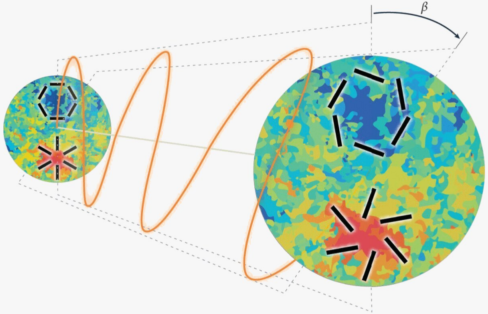

mixing of E and B modes: $\begin{cases} a^E_{\ell m,\mathrm{obs}} = a^E_{\ell m}\cos 2\beta - a^B_{\ell m}\sin 2\beta, \\ a^B_{\ell m,\mathrm{obs}} = a^E_{\ell m}\sin 2\beta + a^B_{\ell m}\cos 2\beta. \end{cases}$

image credit: Yuto Minami.

trying to constrain β

$$\begin{cases} C_{\ell,\mathrm{obs}}^{TT} = C_{\ell,\mathrm{in}}^{TT}, \\ C_{\ell,\mathrm{obs}}^{EE} = \cos^2(2\beta) C_\ell^{EE} + \sin^2(2\beta) C_\ell^{BB} - \sin(4\beta) C_\ell^{EB}, \\ C_{\ell,\mathrm{obs}}^{BB} = \cos^2(2\beta) C_\ell^{BB} + \sin^2(2\beta) C_\ell^{EE} + \sin(4\beta) C_\ell^{EB}, \\ C_{\ell,\mathrm{obs}}^{TE} = \cos(2\beta) C_\ell^{TE} - \sin(2\beta) C_{\ell,\mathrm{i}}^{TB}, \\ C_{\ell,\mathrm{obs}}^{EB} = \sin(4\beta)(C_\ell^{EE} - C_\ell^{BB})/2 + \cos(4\beta) C_\ell^{EB}, \\ C_{\ell,\mathrm{obs}}^{TB} = \sin(2\beta) C_\ell^{TE} + \cos(2\beta) C_\ell^{TB}. \end{cases}$$

$$C_{\ell,\mathrm{obs}}^{EB} = \tan(4\beta)(C_{\ell,\mathrm{obs}}^{EE} - C_{\ell,\mathrm{obs}}^{BB})/2 + \cos(4\beta) C_\ell^{EB}.$$

$$\beta = 0.35 \pm 0.14 \text{ (68\%CL)}$$

Minami and Komatsu (2020) Phys. Rev. Lett. 125

To extract this kind of information from CMB systematics have to be kept under control.

the HWP: reducing systematics

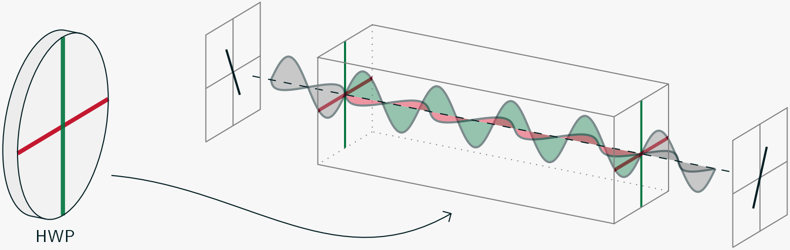

A **rotating** half-wave plate (HWP) as first optical element:

- modulates the signal to $4f_{\mathrm{HWP}}$, allowing to "escape" $1/f$ noise;
- makes possible for a single detector to measure polarization, reducing pair-differencing systematics.

the HWP: inducing systematics

Mueller calculus: radiation described as $S = (I, Q, U, V)$, effect of polarization-altering devices parametrized by $\mathcal{M}$: so that $\mathrm{S}' = \mathcal{M} \cdot \mathrm{S}$.

For an ideal HWP, $\mathcal{M}_{\text{ideal}} = \text{diag}(1, 1, -1, -1)$, but let's look at a realistic case:

$\mathcal{M}_{\text{HWP}} =$

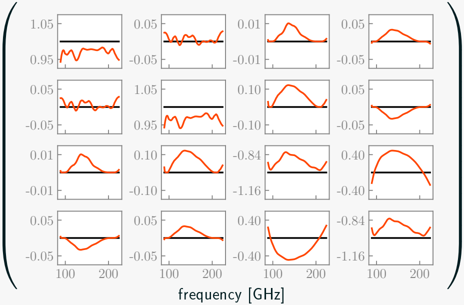

how does this affect the observed maps?

Giardiello et al. (2022) A&A 658

steps we took in that direction

- work on a simulation pipeline for a LiteBIRD-like mission;
- simulate TODs with HWP non-idealities and convert them in maps;
- derive analytical formulae to interpret the output.

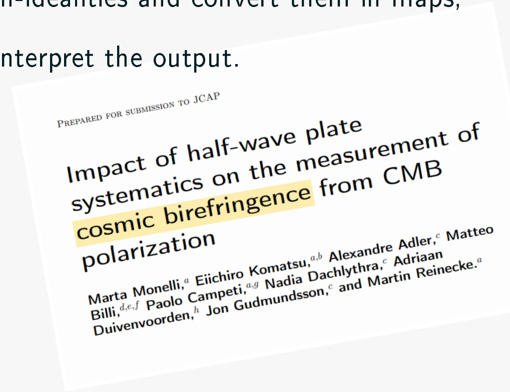

Prepared for submission to JCAP

Impact of half-wave plate systematics on the measurement of cosmic birefringence from CMB polarization

Marta Monelli,[a] Eiichiro Komatsu,[a,b] Alexandre Adler,[c] Matteo Billi,[d,e,f] Paolo Campeti,[a,g] Nadia Dachlythra,[c] Adriaan Duivenvoorden,[h] Jon Gudmundsson,[c] and Martin Reinecke.[a]

Monelli et al. submitted to JCAP, eprint: arXiv:2211.05685

simulations

why do we simulate TOD

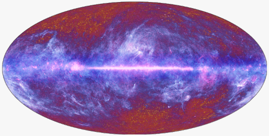

CMB sky maps

image credit: *Planck* collaboration

why do we simulate TOD

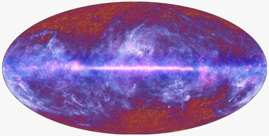

detection

time ordered data (TOD)

map-making

multi-frequency maps

foreground cleaning

CMB sky maps

image credit: *Planck* collaboration

why do we simulate TOD

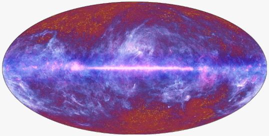

detection

time ordered data (TOD)

map-making

multi-frequency maps

foreground cleaning

CMB sky maps

TOD: collection of the signal detected by *each of the (4508) detectors* during *the whole (3-year) mission*.

image credit: *Planck* collaboration

why do we simulate TOD

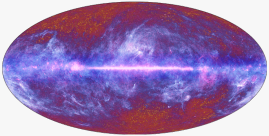

detection

time ordered data (TOD)

map-making

multi-frequency maps

foreground cleaning

CMB sky maps

TOD: collection of the signal detected by *each of the (4508) detectors* during *the whole (3-year) mission*.

Simulating TOD is crucial in the planning of any CMB experiment: helps studying potential systematic effects.

image credit: *Planck* collaboration

sketch of the pipeline

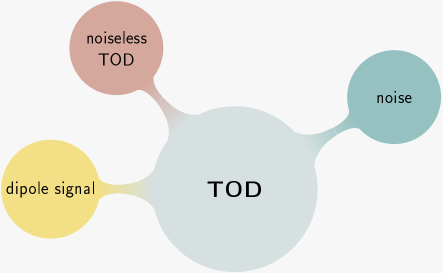

sketch of the pipeline

beamconv: convolution code simulating TOD for CMB experiments with realistic polarized **beams**, scanning strategies and **HWP**.

DUCC: collection of basic programming tools for numerical computation: `fft`, `sht`, `healpix`, `totalconvolve`...

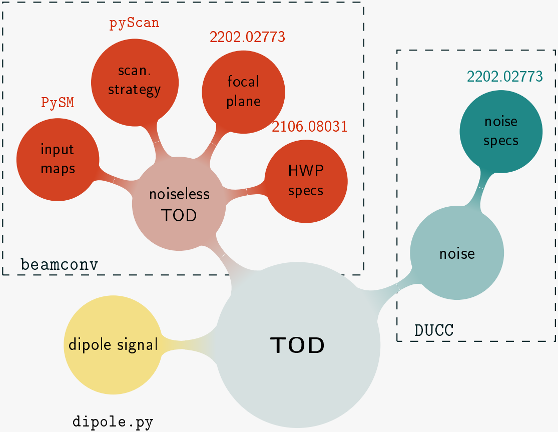

working assumptions

To focus on the impact of **HWP non-idealities**, we consider a simplified problem:

- no noise,
- single frequency,
- CMB-only,
- simple beams,
- HWP aligned to the detector line of sight.

input maps

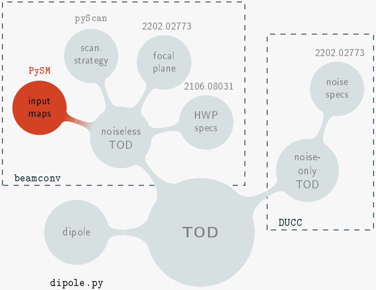

The pipeline can be fed with arbitrary input maps: CMB, foregrounds, or both.

In the paper: I, Q and U input maps with $n_{\mathrm{side}} = 512$ from best-fit 2018 Planck power spectra;

scanning strategy

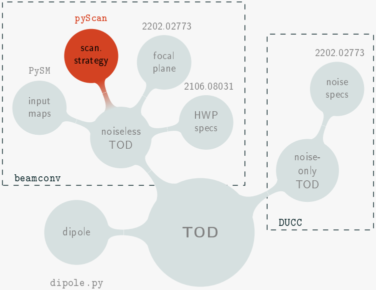

The pipeline can read or calculate pointings. We implemented some functionalities of pyScan in beamconv to deal with satellite missions.

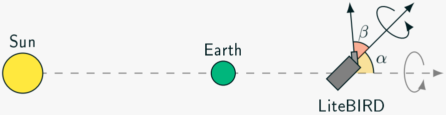

In the paper: 1 year of LiteBIRD-like scanning strategy.

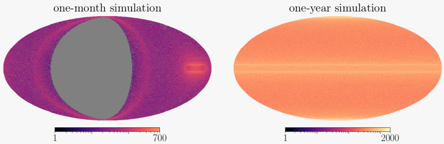

https://github.com/tmatsumu/LB_SYSPL_v4.2

focal plane specifics

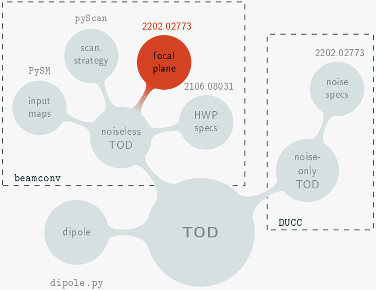

The pipeline can read from the Instrument Model Database (IMO):

```
{'name': 'M02_030_QA_140T',
 'wafer': 'M02',
 'pixel': 30,
 'pixtype': 'MP1',
 [...]
 'pol': 'T',
 'orient': 'Q',
 'quat': [1, 0, 0, 0]}
```

In the paper: 160 dets from M1-140.

specs.	values
f_{samp}	19 Hz
HWP rpm	39
FWHM	30.8 arcmin
offset quats.	[...]

HWP specifics

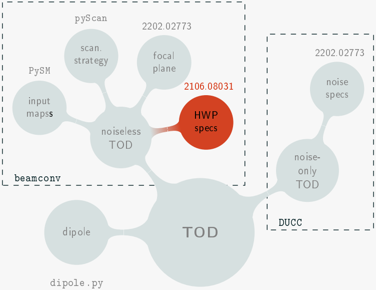

In the paper: HWP is assumed to be ideal in the **first** simulation run (ideal TOD) and realistic in the **second** (non-ideal TOD).

Realistic HWP Mueller matrix elements as shown previously:

$$\mathcal{M}_{\mathrm{HWP}} =$$

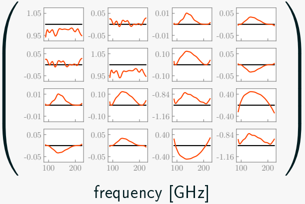

what about maps?

Both ideal and non-ideal TOD processed by **ideal** bin-averaging map-maker.

ideal TOD

non-ideal TOD

ideal map-maker

output = input

potential discrepancies

ideal vs non-ideal output spectra (1)

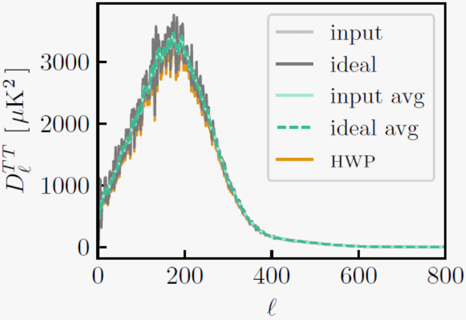

(beam transfer function not deconvolved)

- TT leaked a bit

ideal vs non-ideal output spectra (1)

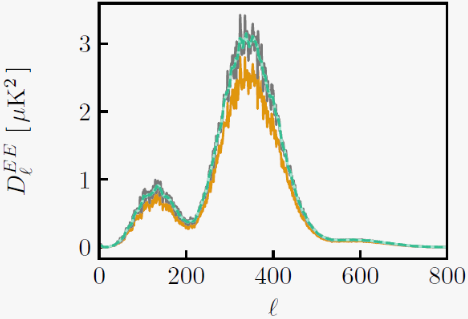

(beam transfer function not deconvolved)

- *TT* leaked a bit
- *EE* leaked a lot!

ideal vs non-ideal output spectra (1)

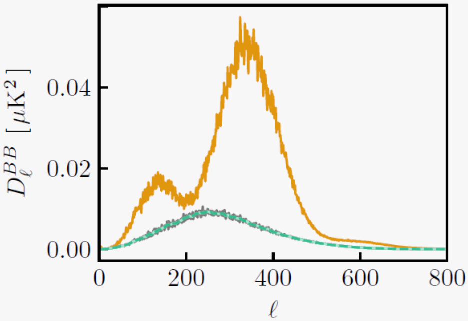

(beam transfer function not deconvolved)

- *TT* leaked a bit
- *EE* leaked a lot!
- *BB* larger (*EE* shape!)

ideal vs non-ideal output spectra (1)

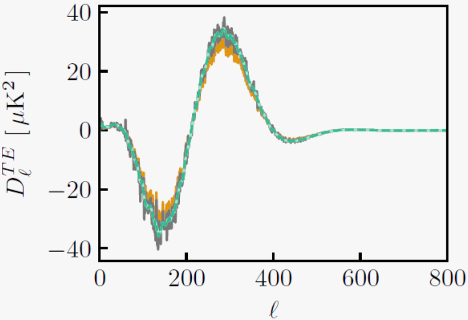

(beam transfer function not deconvolved)

- *TT* leaked a bit
- *EE* leaked a lot!
- *BB* larger (*EE* shape!)
- *TE* leaked a bit

ideal vs non-ideal output spectra (1)

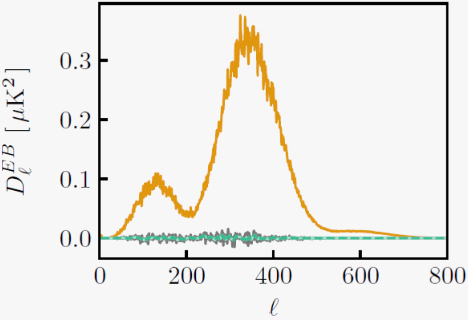

(beam transfer function not deconvolved)

- *TT* leaked a bit
- *EE* leaked a lot!
- *BB* larger (*EE* shape!)
- *TE* leaked a bit
- *EB* non-zero!

ideal vs non-ideal output spectra (1)

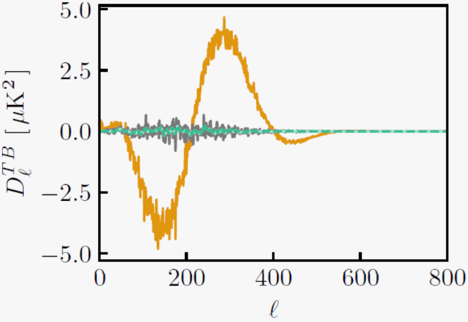

(beam transfer function not deconvolved)

- *TT* leaked a bit
- *EE* leaked a lot!
- *BB* larger (*EE* shape!)
- *TE* leaked a bit
- *EB* non-zero!
- *TB* non-zero!

ideal vs non-ideal output spectra (2)

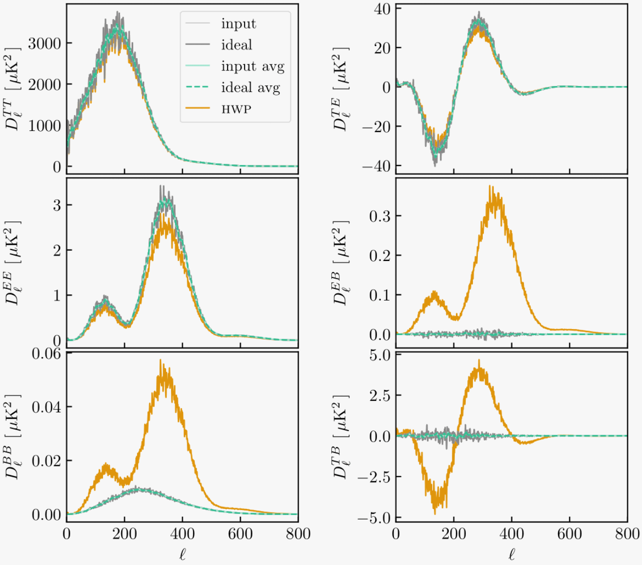

how can we understand this?

modeling the TOD

How beamconv computes the TOD:

$$d_t = \sum_{s\ell m} \left[B^I_{\ell s}\, a^I_{\ell m} + \frac{1}{2} \left({}_{-2}B^P_{\ell s}\, {}_2a^P_{\ell m} + {}_2B^P_{\ell s}\, {}_{-2}a^P_{\ell m} \right) + B^V_{\ell s}\, a^V_{\ell m} \right] \sqrt{\frac{4\pi}{2\ell+1}} e^{-is\psi_t}\, {}_sY_{\ell m}(\theta_t, \phi_t) \,,$$

beam coefficients *(or combinations of them if HWP non-ideal)*.

In the paper: $d = (1\ 0\ 0) \cdot \mathcal{M}_{\text{det}} \mathcal{R}_{\xi-\phi} \mathcal{M}_{\text{HWP}} \mathcal{R}_{\phi+\psi} \cdot \text{S}$.

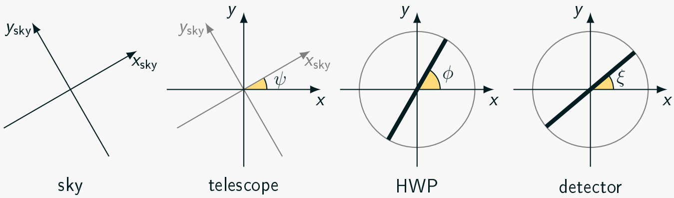

modeling the observed maps

(minimal) TOD: signal detected by 4 detectors.
map-maker: bin-averaging assuming ideal HWP.
estimated output maps: linear combination of $\{I, Q, U\}_{\rm in}$.

$$\begin{pmatrix} d^{(0)} \\ d^{(90)} \\ d^{(45)} \\ d^{(135)} \end{pmatrix} = \begin{pmatrix} (1\ 0\ 0) \cdot \mathcal{M}_{\rm det}\mathcal{R}_{0-\phi}\mathcal{M}_{\rm HWP}\mathcal{R}_{\phi+\psi} \\ (1\ 0\ 0) \cdot \mathcal{M}_{\rm det}\mathcal{R}_{90-\phi}\mathcal{M}_{\rm HWP}\mathcal{R}_{\phi+\psi} \\ (1\ 0\ 0) \cdot \mathcal{M}_{\rm det}\mathcal{R}_{45-\phi}\mathcal{M}_{\rm HWP}\mathcal{R}_{\phi+\psi} \\ (1\ 0\ 0) \cdot \mathcal{M}_{\rm det}\mathcal{R}_{135-\phi}\mathcal{M}_{\rm HWP}\mathcal{R}_{\phi+\psi} \end{pmatrix} \cdot \begin{pmatrix} I_{\rm in} \\ Q_{\rm in} \\ U_{\rm in} \end{pmatrix}$$

Being *ideal*, map-making amounts to apply $(\widehat{A}^T\widehat{A})^{-1}\widehat{A}^T$ to the TOD:

$$\widehat{S} = (\widehat{A}^T\widehat{A})^{-1}\widehat{A}^T A \cdot S.$$

estimated ouput maps

$$
\begin{aligned}
\widehat{I} &= m_{ii} I_{\text{in}} + (m_{iq} Q_{\text{in}} + m_{iu} U_{\text{in}}) \cos(2\alpha) + (m_{iq} U_{\text{in}} - m_{iu} Q_{\text{in}}) \sin(2\alpha)\,, \\
\widehat{Q} &= \frac{1}{2}\Big\{(m_{qq} - m_{uu}) Q_{\text{in}} + (m_{qu} + m_{uq}) U_{\text{in}} + 2 m_{qi} I_{\text{in}} \cos(2\alpha) + 2 m_{ui} I_{\text{in}} \sin(2\alpha) \\
&\qquad + \big[(m_{qq} + m_{uu}) Q_{\text{in}} + (m_{qu} - m_{uq}) U_{\text{in}}\big] \cos(4\alpha) \\
&\qquad + \big[-(m_{qu} - m_{uq}) Q_{\text{in}} + (m_{qq} + m_{uu}) U_{\text{in}}\big] \sin(4\alpha)\Big\}\,, \\
\widehat{U} &= \frac{1}{2}\Big\{(m_{qq} - m_{uu}) U_{\text{in}} - (m_{qu} + m_{uq}) Q_{\text{in}} - 2 m_{ui} I_{\text{in}} \cos(2\alpha) + 2 m_{qi} I_{\text{in}} \sin(2\alpha) \\
&\qquad + \big[-(m_{qq} + m_{uu}) U_{\text{in}} + (m_{qu} - m_{uq}) Q_{\text{in}}\big] \cos(4\alpha) \\
&\qquad + \big[(m_{qu} - m_{uq}) U_{\text{in}} + (m_{qq} + m_{uu}) Q_{\text{in}}\big] \sin(4\alpha)\Big\}\,,
\end{aligned}
$$

where $\alpha = \phi + \psi$. For **good** coverage and **rapidly spinning** HWP:

$$
\boxed{\widehat{\mathsf{S}} \simeq \begin{pmatrix} m_{ii} I_{\text{in}} \\ [(m_{qq} - m_{uu}) Q_{\text{in}} + (m_{qu} + m_{uq}) U_{\text{in}}]/2 \\ [-(m_{qu} + m_{uq}) Q_{\text{in}} + (m_{qq} - m_{uu}) U_{\text{in}}]/2 \end{pmatrix}.}
$$

equations for the $\widehat{C}_\ell$s

Expanding $\widehat{S}$ in spherical harmonics:

$$\begin{aligned}
\widehat{C}_\ell^{TT} &\simeq m_{ii}^2 C_{\ell,\text{in}}^{TT}, \\
\widehat{C}_\ell^{EE} &\simeq \frac{(m_{qq}-m_{uu})^2}{4} C_{\ell,\text{in}}^{EE} + \frac{(m_{qu}+m_{uq})^2}{4} C_{\ell,\text{in}}^{BB} + \frac{(m_{qq}-m_{uu})(m_{qu}+m_{uq})}{2} C_{\ell,\text{in}}^{EB}, \\
\widehat{C}_\ell^{BB} &\simeq \frac{(m_{qq}-m_{uu})^2}{4} C_{\ell,\text{in}}^{BB} + \frac{(m_{qu}+m_{uq})^2}{4} C_{\ell,\text{in}}^{EE} - \frac{(m_{qq}-m_{uu})(m_{qu}+m_{uq})}{2} C_{\ell,\text{in}}^{EB}, \\
\widehat{C}_\ell^{TE} &\simeq \frac{m_{ii}(m_{qq}-m_{uu})}{2} C_{\ell,\text{in}}^{TE} + \frac{m_{ii}(m_{qu}+m_{uq})}{2} C_{\ell,\text{in}}^{TB}, \\
\widehat{C}_\ell^{EB} &\simeq \frac{(m_{qq}-m_{uu})^2-(m_{qu}+m_{uq})^2}{4} C_{\ell,\text{in}}^{EB} - \frac{(m_{qq}-m_{uu})(m_{qu}+m_{uq})}{2} (C_{\ell,\text{in}}^{EE} - C_{\ell,\text{in}}^{BB}), \\
\widehat{C}_\ell^{TB} &\simeq \frac{m_{ii}(m_{qq}-m_{uu})}{2} C_{\ell,\text{in}}^{TB} - \frac{m_{ii}(m_{qu}+m_{uq})}{2} C_{\ell,\text{in}}^{TE}.
\end{aligned}$$

analytical vs non-ideal output spectra

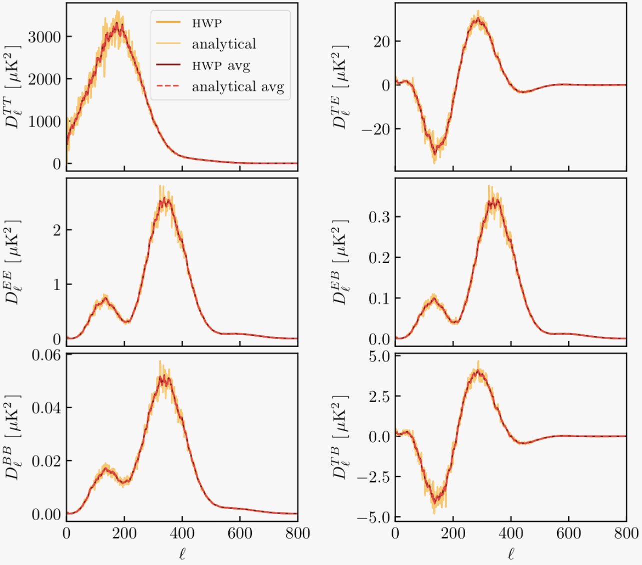

impact on cosmic birefringence

HWP-induced miscalibration

Analytic $\widehat{C}_\ell$s satisfy the relations:

$$\begin{cases} \widehat{C}_\ell^{EB} \simeq \tan(4\widehat{\theta})/2 \left[\widehat{C}_\ell^{EE} - \widehat{C}_\ell^{BB}\right] \\ \widehat{C}_\ell^{TB} \simeq \tan(2\widehat{\theta})\,\widehat{C}_\ell^{TE} \end{cases}$$

The HWP induces an additional miscalibration, **degenerate** with cosmic birefringence and polarization angle miscalibration!

HWP-induced miscalibration

Analytic $\widehat{C}_\ell$s satisfy the relations:

$$\begin{cases} \widehat{C}_\ell^{EB} \simeq \tan(4\widehat{\theta})/2 \left[\widehat{C}_\ell^{EE} - \widehat{C}_\ell^{BB}\right] \\ \widehat{C}_\ell^{TB} \simeq \tan(2\widehat{\theta})\,\widehat{C}_\ell^{TE} \end{cases}$$

our formulae suggest

$$\widehat{\theta} \equiv -\frac{1}{2}\arctan\frac{m_{qu}+m_{uq}}{m_{qq}-m_{uu}} \sim 3.8^\circ,$$

compatibly with simulations.

The HWP induces an additional miscalibration,
degenerate with cosmic birefringence and polarization angle miscalibration!

This doesn't mean that the HWP will keep us from measuring β,
but it shows how important it is to carefully calibrate $\mathcal{M}_{\mathrm{HWP}}$.

simple generalizations

including frequency dependence

How does $d = (1\ 0\ 0) \cdot \mathcal{M}_{\text{det}} \mathcal{R}_{\xi-\phi} \mathcal{M}_{\text{HWP}} \mathcal{R}_{\phi+\psi} \cdot \mathsf{S}$ change when the **frequency dependence** of $\mathcal{M}_{\text{HWP}}$ and signal is taken into account?

$$d = (1\ 0\ 0) \cdot \mathcal{M}_{\text{det}} \mathcal{R}_{\xi-\phi} \int \mathrm{d}\nu \, \mathcal{M}_{\text{HWP}}(\nu) \mathcal{R}_{\phi+\psi} \cdot \mathsf{S}(\nu) \, .$$

Assuming an ideal map-maker and retracing the same steps as before:

$$\widehat{\theta} = -\frac{1}{2} \arctan \frac{\langle m_{qu} + m_{uq} \rangle}{\langle m_{qq} - m_{uu} \rangle}, \qquad \text{where } \langle \cdot \rangle = \int \mathrm{d}\nu \cdot (\nu) S(\nu).$$

instrument miscalibration

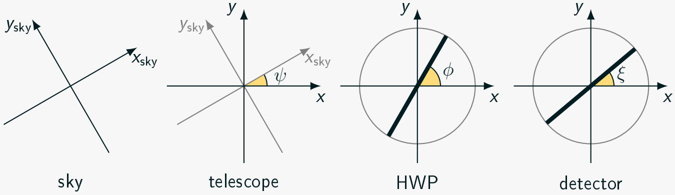

So far, we assumed $\begin{cases} \widehat{\psi} \equiv \psi, \\ \widehat{\phi} \equiv \phi, \\ \widehat{\xi} \equiv \xi, \end{cases}$ but more generally $\begin{cases} \widehat{\psi} \equiv \psi + \delta\phi, \\ \widehat{\phi} \equiv \phi + \delta\psi, \\ \widehat{\xi} \equiv \xi + \delta\xi. \end{cases}$

Taking such (frequency-independent) deviations into account:

$$\widehat{\theta} = -\frac{1}{2} \arctan \frac{\langle m_{qu} + m_{uq} \rangle}{\langle m_{qq} - m_{uu} \rangle} + \delta\theta, \qquad \text{where } \delta\theta \equiv \delta\xi - \delta\psi - 2\delta\phi.$$

steps forward

Even *more general* generalizations worth exploring:

- including a realistic band pass,
- allowing for miscalibrations to depend on ν.

For how long can we push the analytical formulae?

the importance of calibration

how does the map-model change

Without HWP: $$\begin{pmatrix} I_j \\ Q_j \\ U_j \end{pmatrix} = \sum_\lambda g_\lambda \begin{pmatrix} I_\lambda \\ Q_\lambda \\ U_\lambda \end{pmatrix} + n,$$

With HWP: $$\begin{pmatrix} I_j \\ Q_j \\ U_j \end{pmatrix} = \sum_\lambda \begin{pmatrix} g_\lambda^{ii} & 0 & 0 \\ 0 & g_\lambda^{qq-uu} & g_\lambda^{qu+uq} \\ 0 & g_\lambda^{qu+uq} & g_\lambda^{qq-uu} \end{pmatrix} \begin{pmatrix} I_\lambda \\ Q_\lambda \\ U_\lambda \end{pmatrix} + n,$$

where $$g_\lambda = \frac{\int \mathrm{d}\nu\, G(\nu) S_\lambda(\nu)}{\int \mathrm{d}\nu\, G(\nu)}, \quad g_\lambda^{ii} = \frac{\int \mathrm{d}\nu\, G(\nu) m_{ii}(\nu) S_\lambda(\nu)}{\int \mathrm{d}\nu\, G(\nu)},$$ and so on.

HWP non-idealities contribute to gain, polarization-efficiency and cross-polarization leakage.

effective SEDs

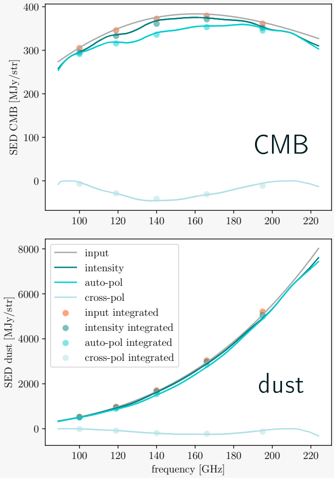

$$\sum_{\lambda} \begin{pmatrix} g_\lambda^{ii} & 0 & 0 \\ 0 & g_\lambda^{qq-uu} & g_\lambda^{qu+uq} \\ 0 & g_\lambda^{qu+uq} & g_\lambda^{qq-uu} \end{pmatrix} \begin{pmatrix} I_\lambda \\ Q_\lambda \\ U_\lambda \end{pmatrix} + n,$$

- Since all these effects are frequency dependent, they affect each component differently,
- An imprecise calibration of $\mathcal{M}_{\mathrm{HWP}}$ can lead to complications in the component separation step.

- we are now provided with a simulation pipeline that can be easily adapted to study more complex problems (adding noise, more realistic beams...);
- the analytical formulae represent an alternative tool to study the same problems more effectively (but approximately);
- obvious application: exploiting the analytical formulae to derive calibration requirements for the HWP Mueller matrix elements, so that they don't prevent us from detecting B-modes, measuring cosmic birefringence, nor spoil the foreground cleaning procedure.